Structural Engineering and Mechanics, *Vol. 67, No. 3 (2018) 233-244*
DOI: https://doi.org/10.12989/sem.2018.67.3.233

Effectiveness of seismic repairing stages with CFRPs on the seismic performance of damaged RC frames

Burak Duran*[1], Onur Tunaboyu[2a], Onur Kaplan[3b] and Özgür Avşar[2c]

[1]*Department of Civil Engineering, Dokuz Eylul University, Tinaztepe Campus, Izmir, Turkey*
[2]*Department of Civil Engineering, Anadolu University, 2 Eylul Campus, Eskisehir, Turkey*
[3]*Earth and Space Sciences Institute, Anadolu University, 2 Eylul Campus, Eskisehir, Turkey*

(Received November 14, 2017, Revised April 25, 2018, Accepted May 13, 2018)

Abstract. This study aims at evaluating the performance of repairing technique with CFRPs in recovering cyclic performance of damaged columns in flexure in terms of structural response parameters such as strength, dissipated energy, stiffness degradation. A 2/3 scaled substandard reinforced concrete frame was constructed to represent the substandard RC buildings especially in developing countries. These substandard buildings have several structural deficiencies such as strong beam-weak column phenomenon, improper reinforcement detailing and poor material properties. Flexural plastic hinges occurred at the columns ends after testing the substandard specimen under both constant axial load and reversed cyclic lateral loading. Afterwards, the damaged columns were externally wrapped with CFRP sheets both in transverse and longitudinal directions and then retested under the same loading protocol. In addition, ambient vibration measurements were taken from the undamaged, damaged and the repaired specimens at each structural repair steps to identify the effectiveness of each repairing step by monitoring the change in the natural frequencies of the tested specimen. The ambient vibration test results showed that the applied repairing technique with external CFRP wrapping was proved to recover stiffness of the pre-damaged specimen. Moreover, the lateral load capacity of the pre-damaged substandard RC frame was restored with externally bonded CFRP sheets.

Keywords: reinforced concrete; CFRP; seismic repairing; ambient vibration; stiffness; flexural damage

1. Introduction

There are many reinforced concrete (RC) frame buildings that need urgent repairing and retrofitting procedures since they are not compatible with modern earthquake codes (Yılmaz and Avşar 2013). Past earthquakes revealed that seismic damages took place especially in substandard buildings, which constitute the major part of existing building stock constructed before 2000s (Tapan *et al.* 2013). These buildings have some deficiencies due to lacking of engineering services, poor quality of materials such as low strength concrete and plain re-bars with improper detailing, improper design and construction applications contrary to earthquake resistant design principles such as strong beam-weak column phenomenon and several structural irregularities (Bal *et al.* 2008). Many substandard RC buildings with their existing conditions do not satisfy the performance criteria and limitations specified in the current seismic codes (Del Vecchio *et al.* 2016). Re-construction of such buildings is both costly and time-consuming. Within this scope, numerous studies have been conducted to improve seismic behavior of RC structures in terms of their structural responses (Yang *et al.* 2015 and Akin *et al.* 2011). In order to improve the structural responses of frames, carbon fiber reinforced polymers (CFRP) have been widely used with the aim of repairing and retrofitting of substandard RC buildings in the last two decades. Fiber reinforced polymers are preferred in structural engineering applications because of their advantages in providing high strength and durability as well as their easy applications.

In structural engineering point of view, many experimental investigations have been conducted to assess the effectiveness of CFRP in enhancing structural characteristics of frames. He *et al.* (2013) conducted an experimental study on RC columns to investigate the repairing technique of large-scaled RC columns with externally bonded CFRPs. Their study showed that the repairing process with CFRPs is effective in enhancing the response parameters such as bending and torsional strength. Balsamo *et al.* (2005) studied on seismic repair of full-scaled RC frame including shear walls by using CFRP composites to investigate its effectiveness. They carried out pseudo-dynamic tests and they indicated that CFRP laminates recovered some significant parameters such as ductility and energy dissipation. Garcia *et al.* (2010) discussed the effect of CFRP materials on the seismic behavior of strengthened substandard RC buildings. They constructed full-scale one-bay two-storey RC frame with poor detailing and they repaired the damaged frame with

*Corresponding author, Graduate Student
E-mail: burak.duran@deu.edu.tr
[a]Ph.D.
E-mail: onurtunaboyu@anadolu.edu.tr
[b]Ph.D.
E-mail: onur_kaplan@anadolu.edu.tr
[c]Associate Professor
E-mail: ozguravsar@anadolu.edu.tr

ISSN: 1225-4568 (Print), 1598-6217 (Online)

externally bonded CFRPs. Their study showed that CFRPs are successful in local strengthening and increasing deformability capacity of columns. Di Ludovico *et al.* (2008) performed an experiment with a full-scale three-storey framed structure to observe the effectiveness of repairing technique with GFRPs by avoiding the brittle collapse modes. They concluded that global deformation capacity of the frame improved by confining the column ends and beam-column joints with GFRP sheets.

Perrone *et al.* (2009) observed that ductility of RC columns can be increased by means of different strengthening techniques including pre-formed CFRP plates. This study demonstrated that the shear strength and ductility of repaired columns can be restored over original capacity of the pre-damaged columns. Furthermore, Wang *et al.* (2016) studied on seismic performance of damaged RC frame strengthened with CFRP sheets by conducting two experiments. The outcomes of this research figured out that CFRP strengthening procedure have strong influence on seismic performance of RC frame in the way of ductility and load bearing capacity of damaged RC frame even though the cracks were not treated.

Sun *et al.* (2011) carried out some experiments to explore the effectiveness of CFRP wrapping technique in rapid repairing severely earthquake-damaged bridge piers with flexural-shear failure mode. This study showed that CFRP material provided higher strength and lateral displacement capacity compared to original one in addition to shifting failure mode to flexure. Tunaboyu and Avşar (2017) conducted an experimental study on 1/3 scaled RC frames having excessive captive column damage due to partial infill walls. They concluded that seismic repairing of captive column damage with CFRP wrapping can recover and even improve the structural response of the original frame. Ilki *et al.* (2004) repaired and retrofitted non-ductile rectangular RC columns with low concrete strength and plain re-bars by applying CFRP jackets. In this study, the CFRP material improved strength and ductility parameters of specimens remarkably by providing sufficient confinement.

In this study, the contribution of different CFRP repairing steps to the rigidity of the frame was determined by ambient vibration measurements. Ambient vibration measurements are based on measuring the responses of the considered objects (buildings, turbine blades, plane wings, automobile parts etc.) to ambient excitations such as traffic, wind, earthquake and their combinations. By means of these measurements, modal parameters of the considered system such as frequencies, mode shapes and damping ratios can be identified (Ewins 1995, Maia and Silva 1997). Ozcelik *et al.* (2015) presented an experimental study including RC frame in laboratory conditions and they conducted different dynamic tests as well as ambient vibration tests to estimate the modal parameters of RC frames. Their measurement results showed that modal identification methods can be used for estimating modal parameters. Arslan and Durmus (2014) determined the dynamic characteristics such as natural frequencies, mode shapes and modal damping ratios of a full scaled, one bay and one story RC frame with low strength concrete for different construction stages (bare frame, brick infilled and brick infilled with plaster) using ambient vibration measurements. The results of this study demonstrated that infill wall and plaster considerably increase the frequencies and the stiffness of the frame. Structural attributes of damaged RC structures can be identified through ambient vibration tests as presented in several studies. Fan and Qiao (2011) summarized a comprehensive review on modal parameter-based damage identification methods. According to their study, although there are some limitations, frequency change-based damage identification method can be applied to quantify damage. Escobar *et al.* (2005) presented a damage detection method based on the transformation matrix that uses the global stiffness matrix of a structure to attain a concentration on the primary degrees of freedom. Damage is expressed in terms of loss of stiffness in the proposed method.

Within the scope of this study, a 2/3 scaled one-bay one-storey substandard RC frame constructed in laboratory conditions to represent substandard RC framed structures having strong beam-weak column phenomenon, low concrete strength and plain reinforcement bars with improper detailing such as transverse re-bars with 90° bended hooks. The specimen was tested under a displacement controlled quasi-static cyclic loading. After formation of plastic hinges at the column ends due to flexural behavior, the damaged specimen was repaired with externally bonded CFRP sheets. Additionally, ambient vibration measurements were carried out on the specimens before and after the tests and also at each repair step in order to determine the effect of the repairing technique to the structural stiffness of the RC frame. The originality of this study is both to examine the contribution of each repairing steps in terms of the variation in natural frequency of the specimen along the frame direction and to explore the effectiveness of externally bonded CFRP sheets in enhancing cyclic properties of damaged substandard RC framed structures having plastic hinges at the column ends. By this way, the ambient vibration results of each step were compared to each other to find out the critical repairing step that contributes the most to the structural stiffness of the damaged RC frame. This information is especially important for the structural engineers during the field applications of the CFRP repairing technique. So that the field engineers can pay special attention to the most critical step to benefit more from the CFRP repairing for the damaged substandard RC frames.

2. Experimental procedures

2.1 Test specimen details

A 2/3 one-bay one-storey substandard RC frame was constructed in the laboratory conditions to represent the seismically deficient RC frames in the building stock of Turkey. The frame doesn't comply with the general design principles of current earthquake codes. It has low strength concrete and plain re-bars without satisfying the code requirements regarding the minimum amount and spacing criteria. Transverse reinforcements have 90° bended hook

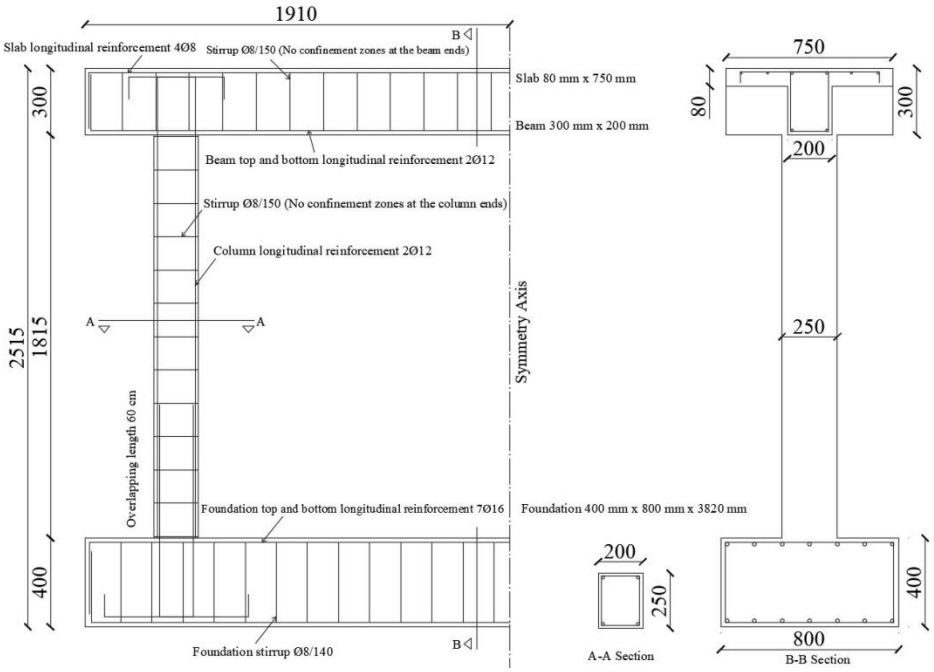

Fig. 1 Reinforcement and geometric details of the frame (Units are in mm)

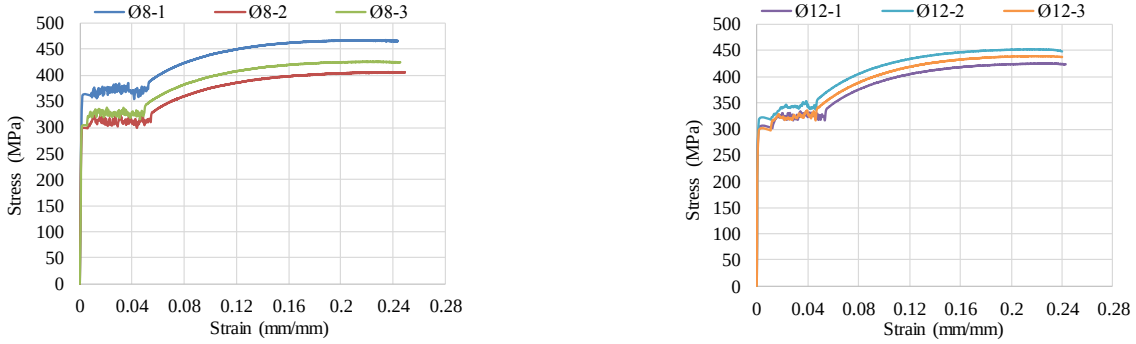

(a) 8 mm reinforcements (b) 12 mm reinforcements

Fig. 2 Tension test results of reinforcement bars

instead of 135°. Also, beam of the tested specimen is stronger than the column. The first test specimen is the reference frame, which is denoted as G1-1. After testing G1-1 specimen, the damaged substandard RC frame, which is denoted as G1-1-CFRP, was repaired with externally bonded CFRP sheets and retested under the same loading conditions.

The column dimensions were 200 mm×250 mm and beam dimensions were designed as a T-section to reflect the contribution of the slab. The beam width and height is 200 and 300 mm, respectively, together with a slab thickness of 80 mm (Fig. 1). The reinforced concrete frame was detailed such that the plastic moment capacity of the beam is higher than the plastic moment capacity of the column, which causes the formation of plastic hinges at column ends. Such detailing is commonly observed in substandard RC frames in the developing countries due to consideration of gravity effects only in the design stage. This application violates the strong column-weak beam principle enforced by the modern seismic codes. Furthermore, low strength concrete and plain re-bars with inadequate detailing are the other deficiencies taken into account in the construction of the test specimen to represent the substandard RC structures.

The aspect ratio of the frame, which is the ratio of the frame height (h) to its width (L), is 0.66. The foundation was designed more rigid than the columns to provide fully restrained support conditions at the bottom ends of columns. The foundation was connected to the strong floor by means of ten bolts to restrict any displacement in any direction.

2.2 Material properties

The frame was constructed and detailed by considering substandard RC frames in Turkey. All the reinforcements used in the construction are plain re-bars. The longitudinal re-bars of the structural components have the diameter of 12 mm. There are no confinement zones at the member ends and all transverse reinforcements of members have 8 mm diameter with 90° bended hooks. The longitudinal reinforcement ratio of the column is 0.9%, which is less than the limiting value of 1% as per TEC (2007). The

(a) Column top end (b) Column bottom end

Fig. 3 Damage view after the first test

concrete compressive strength was selected to be around 10-12 MPa according to Bal *et al.* (2008) to consider the poor concrete quality in substandard RC structures.

Concrete test samples having 150 mm×300 mm cylindrical dimensions taken during the construction of reinforced concrete frame were tested under axial compression to determine their mechanical properties. The average concrete compressive strength was determined as 11.4 MPa at 28 days after casting. Similarly, steel reinforcement samples corresponding to each reinforcement diameter used in the construction were taken to conduct tension test. The approximate yield strength and elasticity modulus of tested samples are almost 330 MPa and 200 GPa according to the axial tension test results, respectively. Besides, the ultimate strength and strain of the steel samples are determined as 435 MPa and 24%, respectively.

The tension test results of reinforcement bars obtained from the steel samples, which their diameters are 8 mm and 12 mm, are shown in Fig. 2.

CFRP sheets were used to repair the damaged RC frame after the first test. There are four components used for repairing process, which are chemical anchorage, primer epoxy coater, epoxy-based repair and anchorage mortar, and resin (saturant). The compressive strength of chemical anchorage is 8.2 MPa and the flexural bending capacity of primer epoxy coater is 20 MPa. Also, compressive strength of the epoxy-based mortar and saturant is 75 MPa and 60 MPa, respectively. The last material used to complete repair process is CFRP sheets having 0.111 mm thickness, 230 GPa modulus of elasticity and 4900 MPa ultimate tensile strength with 2.10% ultimate strain.

2.3 Repair procedure and methodology

Depending on the demands and the failure type of a structure, CFRP sheets can be effective in improving the strength, ductility and energy absorption capacity of columns (Sheikh *et al.* 2002). Within the scope of this study, CFRP material was selected to repair the damaged substandard RC frame whose columns have plastic flexural hinges at the top and bottom ends. The aim of this repairing procedure is to recover the cyclic performance of the substandard RC frame after the damage has been occurred (Fig. 3).

The entire repairing procedure took almost 11 days to conduct the experimental test and involved a total of six steps. In the first step, the column and beam surfaces smoothened and corners were rounded to prevent stress concentrations at sharp edges and to avoid a premature rupture of CFRP sheets. Then, the chemical anchorage was injected to several holes drilled at the plastic hinge zones to fill the cracks. Then primer epoxy coat was applied on the concrete surface of columns to achieve an efficient adhesive between the concrete and epoxy-based repair and anchorage mortar. A total of seven days were waited for hardening process of epoxy coat according to the catalogue. Afterward, the epoxy-based repair and anchorage mortar was applied to the column surfaces with a thickness of 2-3 mm to repair cracks in addition to providing certain degree of bonding between the CFRP sheets and repaired specimens. Before hardening the epoxy-based mortar, firstly the longitudinal CFRP sheets were placed on the two faces of columns by extending over the foundation and beams to provide sufficient bonding. The transverse CFRP sheets were then placed at the top and bottom ends of columns for both confining the column ends and anchoring the longitudinal CFRPs. Before and after placing the CFRP sheets on the surface of the columns, epoxy resin was applied both on the concrete surface and CFRP sheets. Epoxy resin also increases the flexural and shear capacity of the applied members. All these repairing procedures are presented visually in Fig. 4.

The substandard RC frame was exposed to flexural damage during cyclic test and the occurrence of plastic hinge zones at column ends were clearly observed during and after the test. No crack was observed in the beam after the test. This outcome is in compatible with the design of test specimen having strong beam-weak column phenomenon. To be able to improve the cyclic response properties of the frame and provide higher strength compared to the damaged specimen, the CFRP sheets were externally bonded by two layers longitudinally and three layers laterally. The aim for the application of longitudinal CFRP sheets is to recover the moment carrying capacity of the damaged columns having plastic hinges at the ends. Longitudinal CFRP sheets were extended over the beam and foundation at the column top and bottom, respectively. Three layers of transverse CFRP sheets were applied around the column ends with 500 mm height. In addition to the confinement effect of transverse CFRPs, they also have contribution in restraining the debonding between the longitudinal CFRPs and concrete surface. The schematic view of the CFRP sheets is shown in Fig. 5.

2.4 Ambient vibration measurements

Ambient vibration tests were carried out by using four uniaxial, force balanced accelerometers at the two upper ends of the RC frame at the beam and slab level (Fig. 6). Due to presence of externally bonded CFRP sheets on the beams, there were only two accelerometers in the repaired frame at the slab level. The accelerometers were placed at two end points at the slab level for comparison purposes to improve the reliability of the ambient vibration measurement data (Fig. 7). The measurements were taken before and after the two tests to make comparison between the reference frame and the repaired frame with CFRP sheets. These measurements were obtained without any additional mass on the frame, which was connected only to the strong floor during the ambient vibration test measurements.

In addition to 4 measurements taken from both

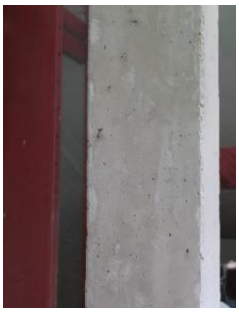

(a) Surface smoothening and rounded edges

(b) Injecting chemical anchorage

(c) Applying primer epoxy coater

(d) Application of epoxy-based repair and anchorage mortar

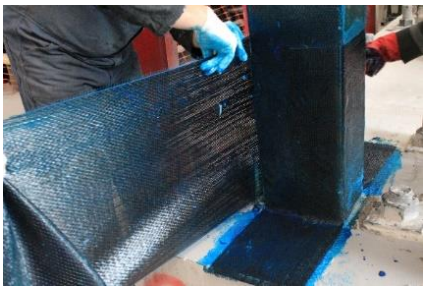

(e) Wrapping CFRP sheets with saturant material

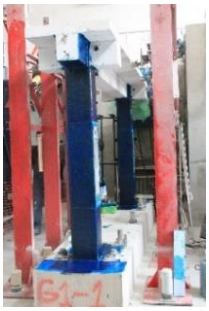

(f) General view of the specimen after completing the repair process

Fig. 4 Repairing procedure for the damaged columns

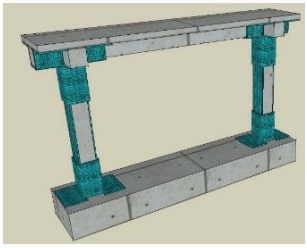

(a) General view

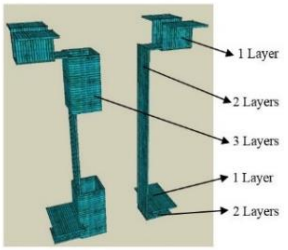

(b) CFRP sheets

Fig. 5 Schematic view of application of CFRP sheets

(a) Front side

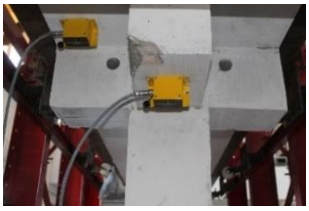

(b) Back side

Fig. 6 Location of accelerometers (G1-1)

(a) Front side

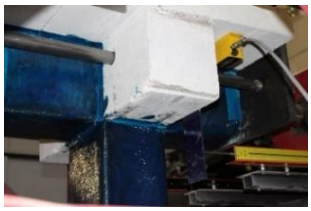

(b) Back side

Fig. 7 Location of accelerometers (G1-1-CFRP)

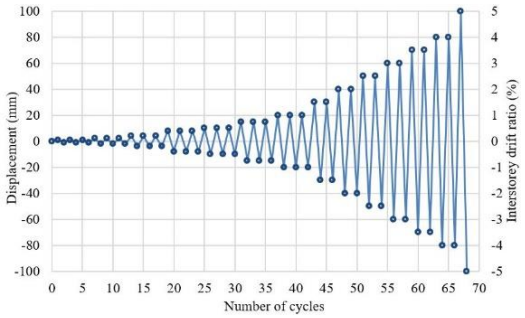

Fig. 8 Loading protocol

specimens before and after testing, additional data were obtained to find out the contribution of each repair step to the structural stiffness. There are totally 17 measurements, performed before and after the application of repair materials, during the waiting period at each day and at the beginning and at the end of the whole process. Enhanced Frequency Domain Decomposition Technique (EFDD) was used to obtain the natural frequencies of the RC Frame.

2.5 Test system and loading procedure

A reversed cyclic lateral displacement protocol (Fig. 8) was applied to the substandard RC frame to investigate several response parameters such as strength, stiffness and energy dissipation. This loading protocol includes critical inter-storey drift ratio limits indicated in seismic design and assessment chapters of TEC (2007). Strain gauges were placed on the longitudinal re-bars and stirrups to record axial deformations in the reinforcement bars of the critical RC sections (Fig. 9).

The RC frame to be tested under the reversed cyclic loading through MTS actuator was connected to the strong floor. Steel plates were used to apply constant axial load on

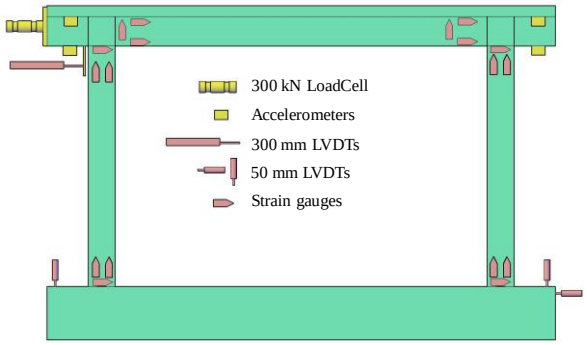

Fig. 9 Instrumentation of the tested specimen and their locations

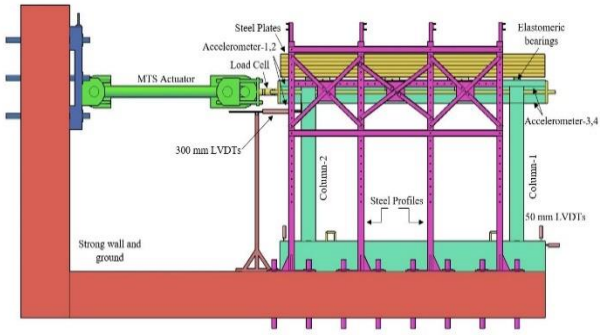

Fig. 10 Schematic view of the experimental setup

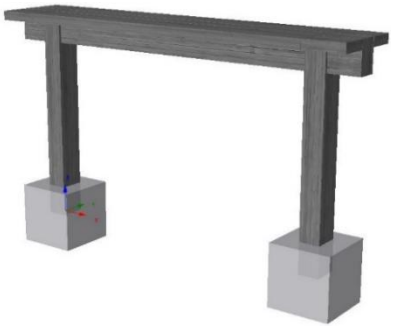

Fig. 11 3D view from the analytical model of the reference frame in SeismoStruct

the columns. The constant axial load, which was applied to the column ends, is equal to 0.1*fc*Ac where f_c is the average concrete compressive strength and A_c is the gross section area of the column. This load level is the minimum axial force limit specified in TEC (2007) for columns. Further axial load level couldn't be applied because of limited laboratory capacity and safety concerns. Steel plates were supported by elastomer bearings, which were placed over columns, not to introduce additional stiffness from steel plates to the RC frame. Also, roller supports were provided by a wheel system at both sides of the slab to prevent out-of-plane movement of the RC frame under the combined effect of lateral and vertical load. There are totally five displacement transducers, two of which measure the lateral displacements of the frame and rest of them measure the lateral movement and rotation of the foundation, if any. The general view of the experimental setup is shown in Fig. 10.

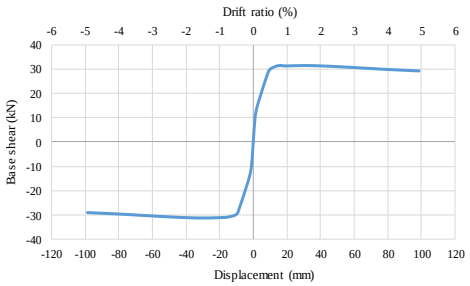

Fig. 12 Capacity curve of the reference frame

2.6 Analytical model

The analytical model was constructed before the tests to make verification between the expected behavior and observed behavior in real tests. SeismoStruct version 7.0.6 was used to develop the analytical model of the reference frame. The RC sections were modelled with fiber sections to be employed in inelastic forced-based frame element, which considers a distributed plasticity among the integration points along the RC member. A bilinear material model was adopted for reinforcement steel. Mander *et al.* (1988) concrete nonlinear model was used for confined and unconfined concrete. In addition to material nonlinearity, geometric nonlinearity was also taken into account in the analysis. Static time-history analysis was conducted after the application of gravity loading on the RC frame. Lateral cyclic displacements presented in Fig. 8 were applied at the beam level during the static time-history analysis to be compatible with the displacements recorded during the test. The general perspective view from the analytical model of the reference frame is shown in Fig. 11.

After conducting static time history analysis along with gravity loads, the capacity curve of the frame corresponding to base shear vs. displacement was obtained as shown in Fig. 12. Therefore, the lateral load capacity of the reference frame was obtained as 31 kN and 30.8 kN in forward and backward directions, respectively. Analytically obtained load capacity is in good agreement with the experimental result presented in Fig. 14(b). Also, it is important that a ductile behavior was also observed by the conducted analysis in accordance with the experimental observation since the reinforcements were yielded before crushing of concrete. Moreover, the unconfined concrete crushed in both ends of two columns together with yielding of reinforcements according to the performed cyclic analysis.

The strain distribution of unconfined concrete and longitudinal reinforcements of columns at the bottom ends are given in Fig. 13. The ultimate strain of unconfined concrete was taken as -0.005 according to the TEC (2007), while the yield strain of the re-bars was determined to be 0.0016, which is the average yield strain obtained from the rebar tension tests shown in Fig. 2(b). Considering below Fig. 13, it is observed that the longitudinal reinforcements were yielded in the first cycles of the test. This observation is in accordance with the flexural cracks at the column ends occurred during the test (Figs. 3 and 17). Whereas, the unconfined concrete at the extreme fiber of the column section reached its ultimate strain value towards the end of

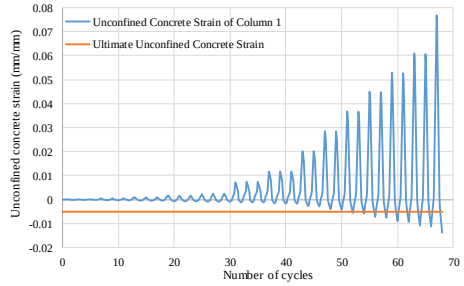

(a) G1-1_Column 1 (Unconfined concrete strain)

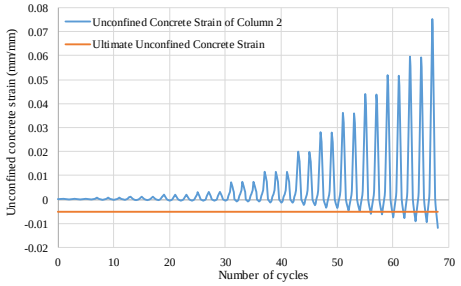

(b) G1-1_Column 2 (Unconfined concrete strain)

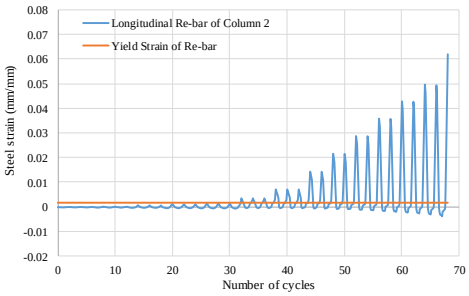

(c) G1-1_Column 1 (Reinforcement bar strain)

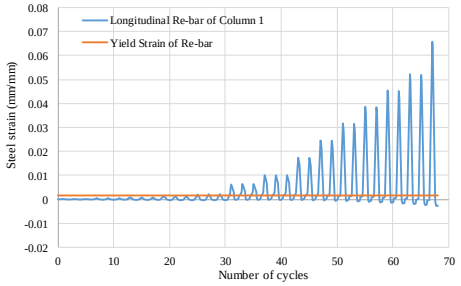

(d) G1-1_Column 2 (Reinforcement bar strain)

Fig. 13 Variation in material strains

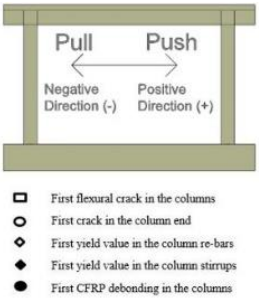

(a) General notations

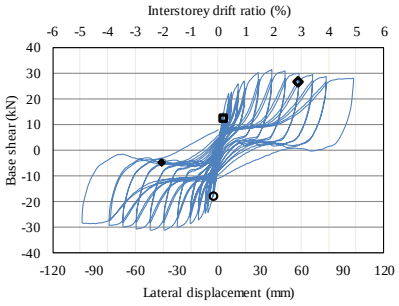

(b) G1-1

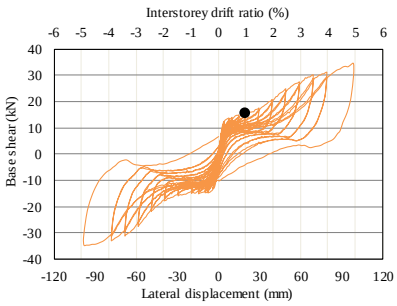

(c) G1-1-CFRP

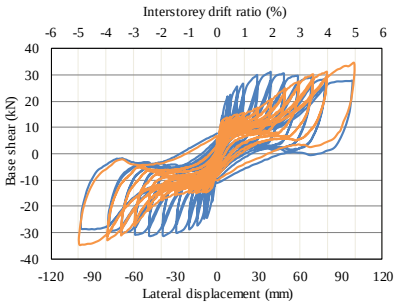

(d) Comparison

Fig. 14 Hysteretic loops of the specimens

the cyclic test. This verifies the ductile response of the RC frame.

Crushing of cover concrete was also observed in the test as shown in Fig. 3(b) over the wide flexural crack, which was already occurred in the previous cycle. Moreover, beam sections did not attain their yield capacity according to analysis results. Therefore, all the nonlinearity was concentrated at the column ends as occurred in the tests (Figs. 3 and 17).

3. Results

3.1 Frame test results

The overall performance of tested specimens and comparisons between the results are presented in the following section. The ultimate lateral load for the first reference frame (G1-1) was measured as 31.2 kN. The test was terminated at the top displacement of 98 mm (5% drift ratio). As calculated and predicted before the test, flexural behavior dominated the overall response of RC frame and strong beam-weak column phenomenon was observed by formation of plastic hinges at column ends. During the test, a ductile behavior was observed on the frame members

under constant axial load and reversed cyclic lateral displacements. The maximum crack width was measured as 7 mm at the end of the test in the column ends.

The second specimen is called as G1-1-CFRP, repaired with CFRP sheets by wrapping the column members. The repaired frame was also tested with the same loading protocol and reached more ultimate load than the bare frame with 34.5 kN at 5% drift ratio. CFRP repairing procedure increased the lateral load capacity of the damaged substandard RC frame compared to the undamaged bare frame especially in the higher drift ratios.

Although yield strength of repaired frame is less than G1-1, the ultimate load capacity of the G1-1-CFRP is greater than the bare frame. The CFRP sheets on the foundation at the column bottom ends swelled at the top displacement of 19.70 mm (1% drift ratio) and hence separation was observed between CFRP sheet and concrete surface.

The hysteretic responses of the tested specimens are shown in Fig. 14. It was observed during the test that there was no crack or any damage in the beam. Also, the strain values of reinforcements obtained from strain gauges indicate that any re-bar of the beam member didn't reach the yield value. On the contrary, the longitudinal re-bar and stirrup of column members yielded at +2.93% and -2% drift ratio, respectively. The first flexural crack in the column members formed at +0.2% drift ratio. For the second repaired frame, the CFRP debonding occurred at +1% drift ratio at the column bottom ends.

During the cyclic response, it was observed that after reaching higher drift ratios, the residual lateral load capacity of the damaged specimen was less than 10 kN when the specimen is at its un-deformed position due to the accumulation of damage. The yielding lateral load capacity of the repaired specimen reached to 13 kN, which is almost 50% higher than the residual load capacity of the damaged specimen. Moreover, as the drift ratio increases, both longitudinal and transverse CFRP sheets became effective and the lateral load capacity of the repaired specimen increased up to the value greater than the one for reference specimen. Due to the limitation in the stroke capacity of the hydraulic jack, the tests were ended at 5% drift ratio. However, the increasing trend even at 5% drift ratio in the hysteresis curve of G1-1-CFRP specimen in Fig. 14(c) can be accepted as an indicator for larger displacement capacity.

The increased drift capacity of the repaired frame can be attributed to the confinement effect of transverse CFRP sheets. Similarly, Ilki *et al.* (2018) presented an experimental study on the retrofitting of a substandard RC building with CFRP wrapping for columns only. Confinement effect of CFRP wrapping on the columns has a significant contribution on the lateral displacement capacity of retrofitting frame.

Damage pattern of the tested specimens are shown in Figs. 15 and 16. Both reference and repaired frame was tested up to 5% inter-storey drift ratio and the views from the critical drift ratio limits are shown in the following figures.

The shear capacity of each column was calculated according to Turkish Earthquake Code (TEC 2007) with Eq. (1). The equation includes tensile strength of

(a) G1-1 (b) G1-1-CFRP

Fig. 15 Damage pattern of the tested specimens at +2% drift

(a) G1-1 (b) G1-1-CFRP

Fig. 16 Damage pattern of the tested specimens at +5% drift

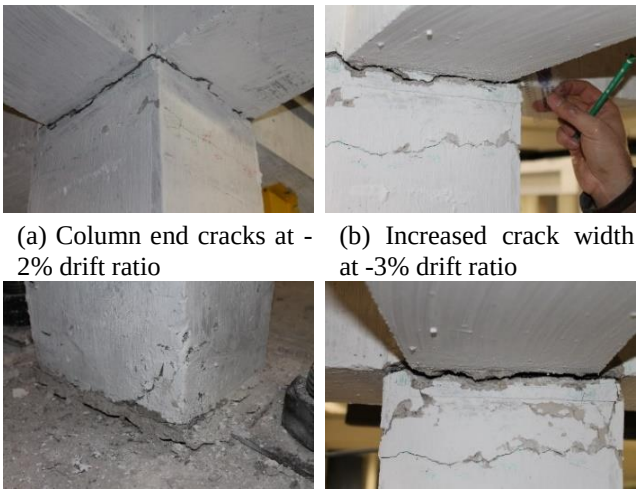

(a) Column end cracks at -2% drift ratio

(b) Increased crack width at -3% drift ratio

(c) Column bottom end at +3.5% drift ratio

(d) Plastic hinge at the column top end at 5% drift ratio

Fig. 17 Critical damage views of the G1-1

concrete (f_{ct}), width of column (b_w), effective height of the cross section (d), axial load applied to the column (N_d), gross section area of column (A_c), number of stirrup arms at a section (n), area of the lateral reinforcement (A_0), spacing of lateral reinforcement (s) and yield strength of lateral reinforcement (f_{yw}). The shear capacity of one column is calculated as 48.6 kN, while the total shear capacity of the frame will be 97.2 kN corresponding to column shear failure. When the ultimate load of the tested specimens obtained from the hysteretic curves (Fig. 14) was compared with the total shear capacity of the frames, it was observed that the total shear capacity of the frame is almost three times larger than its lateral load capacity. This clearly indicates that the overall response of the tested specimens was dominated by the flexural response. Therefore, a brittle type of shear failure wasn't observed during the test.

$$V_r = \left[0.52 \times f_{ct} \times b_w \times d \times \left(1 + 0.07 \times \frac{N_d}{A_c}\right)\right] + \left[\frac{n \times A_0}{s} \times f_{yw} \times d\right] \quad (1)$$

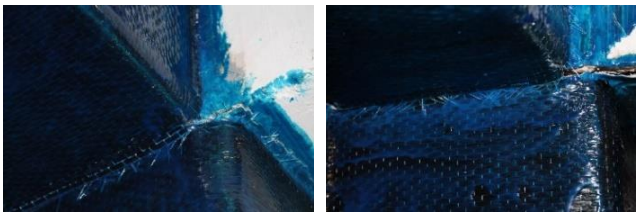

(a) CFRP rupture at -2.5% drift ratio

(b) Stress concentration in CFRP sheets at +3.5% drift ratio

(c) CFRP swelling at the foundation at +3.5% drift ratio

(d) CFRP rupture and debonding at -5% drift ratio

Fig. 18 Critical damage views of the G1-1-CFRP

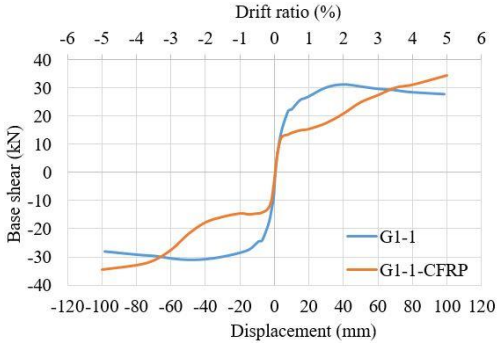

Fig. 19 Envelope curves for hysteretic loops

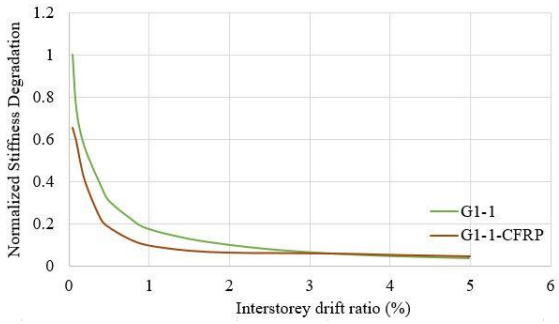

Fig. 20 Stiffness degradation curves

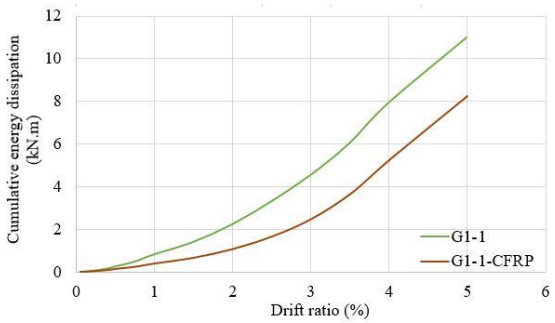

Fig. 21 Cumulative energy dissipation capacity of the tested specimens

Based on the design principles of the RC frame, where the plastic moment capacity of T-sectioned beam is larger than the column members, beam member had no crack or visible damage in contrast to column members. As can be seen in Fig. 17, the column ends were exposed to severe damage and formation of plastic hinges was clearly observed as the lateral displacement progress.

The first frame has large cracks at the column ends due to bending moment. After observing first bending crack at +0.2% drift ratio, the width of the cracks increased and new cracks occurred almost 10 cm away from the column top ends that is almost equal to the plastic hinge length of the column. The substandard reinforced concrete frame reached its flexural moment capacity at 2% drift ratio and then the ultimate load decreased smoothly until the end of test. The second frame, which was repaired with CFRP sheets, had first CFRP rupture starting around at 1% drift ratio. Swellings on the CFRP sheets were observed together with CFRP rupture (Fig. 18). The repaired frame had significant separations at the joints when the experiment reached its maximum drift ratio limit. At the ends of column members, the transverse CFRP sheets also worked effectively and swelling in CFRP sheets was observed. It should be also underlined that the plastic hinging is not transferred to the beam due to the fact that the plastic moment capacity of T-shaped beam section is relatively higher than the column sections. Moreover, as shown in Fig. 5, longitudinal CFRP sheets were extended to the beam ends, which also improved the moment capacity of the beam end sections.

The hysteretic behavior of the RC frames and some critical failure types at the local level are indicated on the hysteretic curves for the two test specimens (Fig. 14). Envelope curves are obtained by connecting the ultimate lateral load values at the target lateral displacement points at the first peak of each cycle (Fig. 19). The ultimate loads of the reference and repaired specimens are 31.2 kN and 34.5 kN, respectively. After 2% drift ratio, lateral load capacity of G1-1 decreased smoothly to 28.5 kN. On the other hand, the repaired frame continuously increased its lateral load capacity after 0.5% drift ratio**.**

The lateral stiffness of the tested specimens diminishes as the lateral displacements increases because of the plastic deformations and the formation of cracks on the structural members. In order to determine the stiffness degradation of the frames, peak-to-peak stiffness was calculated for each displacement cycle. It is defined as the slope of the line between peak lateral load values corresponding to the same displacement value for both positive and negative cycle. The peak-to-peak stiffness is normalized with respect to the one for reference specimen for the first cycle. It means that the first peak-to-peak stiffness value of the reference frame corresponds to the first cycle is accepted as 1 and other stiffness values for the rest of the cycles were normalized with respect to this value. As indicated in Fig. 20, the first reference frame has larger stiffness value at the beginning of the experiment. But, the second repaired frame had almost the same stiffness after 2.5% drift ratio. The damaged frame of G1-1 had large cracks due to plastic deformations at the column ends and the entire repairing process couldn't recover the initial peak-to-peak stiffness of G1-1-CFRP.

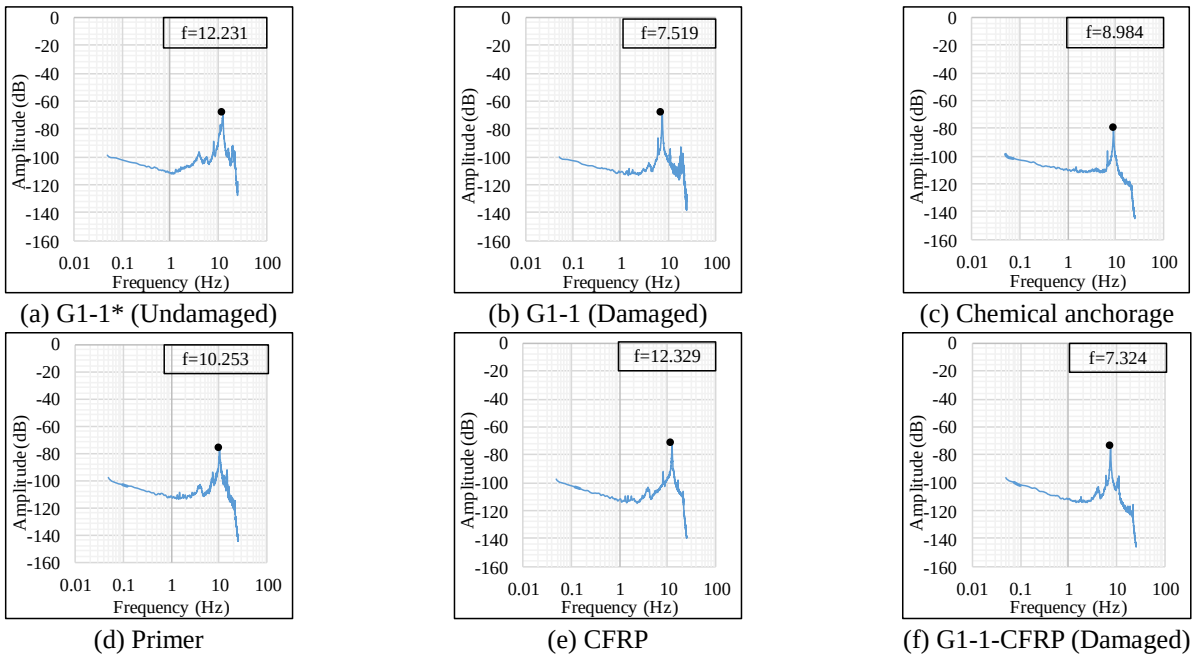

(a) G1-1* (Undamaged) (b) G1-1 (Damaged) (c) Chemical anchorage

(d) Primer (e) CFRP (f) G1-1-CFRP (Damaged)

Fig. 22 Graphical results of ambient vibration tests

The energy dissipation capacity of the tested specimens in each cycle are calculated by considering the area enclosed within the hysteretic loops of frames for the first cycles of displacement protocol (Fig. 21). The cumulative energy dissipation is then calculated by summing up the areas calculated for each loading cycle. The dissipated energy by the reference frame is 33% larger than the repaired frame in general. This difference is due to large crack widths and compression failure of concrete in the column ends occurred after the first testing.

3.2 Ambient vibration test results

Ambient vibration measurements were taken on the test specimens at various stages to determine the change in the structural stiffness of RC frames. Although such measurements were taken for very small displacement amplitudes and do not represent the seismic response of the frame under severe seismic excitations, they are commonly used for identifying dynamic characteristics of structures.

The ambient vibration measurements include undamaged and damaged conditions for the reference and repaired specimens. Moreover, measurements were taken for each application step during the structural repairing with CFRPs. The obtained data was analyzed, and it was classified into three categories in order to present significant changes and contributions to the structural stiffness. These are the application of chemical anchorage, primer and CFRP. In the following three tables (Tables 1-3), the first frequency value was accepted as the reference value to reflect the change in frequency ratio.

As shown in Fig. 22, the test specimen G1-1* (undamaged) and G1-1 (damaged) has the fundamental frequency of 12.231 Hz and 7.519 Hz, respectively before and after the tests. As expected, the decrease in the frequency is an evidence for the softening of the specimen due to the imposed damage. After the test, fundamental frequency of the specimen increased to 8.984 Hz by the application of chemical anchorage. The fundamental frequencies obtained after applying primer epoxy coating and CFRP wrapping stages are presented in Tables 1-2, respectively. The primer epoxy coating process has totally 4 measurements in 3 days while the CFRP wrapping procedures have 8 measurements in 7 days. The first measurements for both stages were monitored in the first day of their applications. It should be noticed that the last measurement of the CFRP wrapping procedure reflects the fundamental frequency of the repaired frame before the second test was performed. The illustrated data showed that all repairing steps increased the frequency of the RC frame.

Table 1 Primer epoxy coating procedure results

	Frequency (Hz)	Variation in Frequency (%)
Primer-1	8.911	0
Primer-2	9.985	+12.1
Primer-3	10.009	+12.3
Primer-4	10.253	+15.1

Table 2 CFRP wrapping procedure results

Measurement No	Frequency (Hz.)	Variation in Frequency (%)
1	10.058	0
2	11.840	+17.7
3	12.036	+19.7
4	12.011	+19.4
5	12.182	+21.1
6	12.255	+21.8
7	12.329	+22.6
8	12.329	+22.6

Table 3 Variation in the frequency measurements for the entire repairing procedure

	Frequency (Hz)	Variation in Frequency (%)
G1-1*	12.231	0
G1-1	7.519	-38.5
Chemical Anchorage	8.984	-26.5
Primer	10.253	-16.2
CFRP	12.329	+0.8
G1-1-CFRP	7.324	-40.1

G1-1*: Undamaged case; G1-1 and G1-1-CFRP: damaged cases

So, the increase in the frequency means that the structural stiffness of the G1-1-CFRP improved with the applied repair steps. The CFRP wrapping step has more contribution on the structural stiffness compared to the primer epoxy coating based on first frequency values of these steps. According to Table 1, three days waiting for the primer epoxy coating is sufficient, while at least 4 days are required to achieve an acceptable level of performance for the CFRP wrapping.

The ambient vibration results obtained from entire repairing procedure was summarized in Fig. 22 and Table 3. In this figure and table, only the last measurement value of each step is presented. According to Table 3, it is seen that the CFRP wrapping stage contributes the most on the structural stiffness of the damaged specimen among the stages of the proposed repairing scheme. Another prominent outcome of Table 3 is that by repairing the damaged substandard RC frame with CFRP wrapping, structural stiffness can be recovered fully compared to the stiffness of the frame before it was tested. This outcome is not in compatible with the normalized peak-to-peak stiffness values presented in Fig. 20. This is due to the fact that ambient vibration tests were conducted on specimens without any lateral displacements. However, even in the first cycle, peak-to-peak stiffness calculation possess some level of imposed damage with the applied lateral displacement. As it can be seen in Fig. 20, the peak-to-peak stiffness degrades very sharply in the first cycles. Therefore, the variation in stiffness calculated by the ambient vibration tests and peak-to-peak stiffness calculated from the cyclic response differ from each other inevitably.

4. Conclusions

This study focused on repairing procedure with CFRP sheets and its influence on the structural response of substandard RC frames having flexural damages. Besides this, the main contribution of this study is to investigate the influence of structural repairing steps on the structural behavior of a damaged substandard RC frame in terms of structural stiffness. For this purpose, ambient vibration tests were conducted on the test specimens in order to explore the change in its natural frequency before and after damage, and also at each repairing step. A 2/3 scaled one-bay one-storey substandard RC frame was constructed in the laboratory conditions. Low concrete strength, plain re-bars with improper reinforcement details were used to represent substandard RC framed structures. Two specimens were tested, the first one is the reference frame (G1-1) and the last one is the repaired frame (G1-1-CFRP). The reference frame firstly tested under both axial load and reversed cyclic displacements. Next, the damaged specimen structurally repaired with externally bonded CRFP sheets by wrapping column members in both longitudinal and transverse directions. Since the flexural behavior dominated the overall response with the formation of plastic hinges at columns ends, no shear failure was observed in both tested specimens.

• The analysis results of the analytical model for the reference frame is in good agreement with the experimental results in terms of ultimate load and strain distribution. In addition, experimentally observed behavior of the reference specimen was also verified with the analysis results of the analytical model, such as formation of plastic hinges at the column ends in the substandard RC frame.

• The structural repairing scheme with CFRP sheets by wrapping the column members was satisfactory in terms of lateral load capacity of substandard RC frame. Lateral load capacity of the damaged RC frame was recovered and even improved with the applied repairing technique especially in the higher drift ratios. The cumulative dissipated energy capacity of the repaired frame is lower than the one for reference specimen due to the presence of plastic hinges at the columns ends. Additionally, the initial stiffness of the repaired frame is lower than the reference frame. The peak-to-peak stiffness degraded due to the imposed structural damage during the test.

• The most remarkable contribution of the applied repairing scheme is the improvement in the displacement capacity of the repaired frame. External wrapping of column ends with transverse CFRP sheets provided additional confinement for the columns and hence improved the displacement capacity of repaired frame. This resulted in an increasing trend in the hysteresis curve of the repaired frame even at 5% drift ratio. On the other hand, displacement demand on the repaired frame will be more due to reduced initial stiffness and yield capacity of the repaired frame compared to original frame.

• The ambient vibration results showed that the entire repair process with CFRP provided a full recovery in the structural stiffness. The fundamental frequency of the repaired frame before the second test was measured to be greater than the undamaged case of G1-1. The practicing engineer should pay much attention on the critical repair stage to take further advantage of the CFRP repairing for the damaged substandard RC frames. Based on the tested specimen, it was found out that the CFRP wrapping stage is the most critical one, which contributes the most on the structural stiffness.

• After testing both specimens, the damaged cases of G1-1 and G1-1-CFRP have almost the same natural frequency. This indicates that externally bonded CFRP wrapping was satisfactory until the end of the experiment and the frame returned to its damaged condition when the specimen is at its original undeformed position, at which the CFRP wrapping was not effective due to partial rupture of CFRP and debonding.

Acknowledgments

The research described in this paper was financially supported by the Scientific Research Commission of Anadolu University with the grant number 1606F552.

References

Akın, E., Canbay, E., Binici, B. and Özcebe, G. (2011), "Testing and analysis of infilled reinforced concrete frames strengthened with CFRP reinforcement", *J. Reinf. Plast. Compos*., **30**(19), 1605-1620.

Arslan, M.E. and Durmus, A. (2014), "Modal parameter identification of in-filled RC frames with low strength concrete using ambient vibration", *Struct. Eng. Mech.*, **50**(2), 137-149.

Bal, I.E., Crowley, H., Rui Pinho, H.R. and Gulay, G. (2008), "Detailed assessment of structural characteristics of Turkish RC building stock for loss assessment models", *Soil Dyn. Earthq. Eng*., **28**(10-11), 914-932.

Balsamo, A., Colombo, A., Manfredi, G., Negro, P. and Prota, A. (2005), "Seismic behavior of a full-scale RC frame repaired using CFRP laminates", *Eng. Struct.*, **27**(5), 769-780.

Ewins, D.J. (1995), *Modal Testing: Theory and Practice*, John Wiley & Sons, New York, U.S.A.

Del Vecchio, C., Di Ludovico, M., Prota, A., Cosenza, E. and Manfredi, G. (2016), "Correlation of in-situ material characterization tests and experimental performances of RC members", *Proceedings of the Italian Concrete Days Giornate AICAP 2016 Congress C.T.E.*, Rome, Italy, October.

Di Ludovico, M., Prota, A., Manfredi, G. and Cosenza, E. (2008), "Seismic strengthening of an under-designed RC structure with FRP", *Earthq. Eng. Struct. Dyn.*, **37**(1), 141-162.

Escobar, J.A., Sosa, J.J. and Gómez, R. (2005), "Structural damage detection using the transformation matrix", *Comput. Struct.*, **83**(4), 357-368.

Fan, W. and Qiao, P. (2011), "Vibration-based damage identification methods: A review and comparative study", *Struct. Health Monitor.*, **10**(1), 83-111.

Garcia, R., Hajirasouliha, I. and Pilakoutas, K. (2010), "Seismic behaviour of deficient RC frames strengthened with CFRP composites", *Eng. Struct.*, **32**(10), 3075-3085.

He, R., Sneed, L.H. and Belarbi, A. (2013), "Rapid repair of severely damaged RC columns with different damage conditions: An experimental study", *Int. J. Concrete Struct. Mater.*, **7**(1), 35-50.

Ilki, A., Tezcan. A., Koç, V. and Kumbasar, N. (2004), "Seismic retrofit of non-ductile rectangular reinforced concrete columns by CFRP jacketing", *Proceedings of the 13th World Conference on Earthquake Engineering*, Vancouver, Canada, August.

Ilki, A., Tore, E., Demir, C. and Comert, M. (2018), *Code Based Performance Prediction for a Full-Scale FRP Retrofitted Building Test*, Seismic Hazard and Risk Assessment, 467-477.

Mander, J.B., Priestley, M.J.N. and Park, R. (1988), "Theoretical stress-strain model for confined concrete", *J. Struct. Eng.*, **114**(8), 1804-1826.

Maia, N.M.M. and Silva, J.M.M. (1997), *Theoretical and Experimental Modal Analysis*, John Wiley and Sons, Inc., New York, U.S.A.

Ozcelik, O., Amaddeo, C., Misir, S., Durmazgezer, E. and Yücel, U. (2015), "Modal identification results of RC frames at different damage levels", *Proceedings of the 3rd Conference on Smart Monitoring Assessment and Rehabilitation of Civil Structures*, Antalya, Turkey, September.

Perrone, M., Barros, J.A. and Aprile, A. (2009), "CFRP-based strengthening technique to increase the flexural and energy dissipation capacities of RC columns", *J. Compos. Constr.*, **13**(5), 372-383.

SeismoSoft (2011), *SeismoStruct-A Computer Program for Static and Dynamic Nonlinear Analysis of Framed Structures*, <www.seismosoft.com>.

Sheikh, S.A. (2002), "Performance of concrete structures retrofitted with fibre reinforced polymers", *Eng. Struct.*, **24**(7), 869-879.

Sun, Z., Wang, D., Du, X. and Si, B. (2011), "Rapid repair of severely earthquake-damaged bridge piers with flexural-shear failure mode", *Earthq. Eng. Eng. Vibr.*, **10**(4), 553-567.

Tapan, M., Comert, M., Demir, C., Sayan, Y., Orakcal, K. and Ilki, A. (2013), "Failures of structures during the October 23, 2011 Tabanlı (Van) and November 9, 2011 Edremit (Van) earthquakes in Turkey", *Eng. Fail. Analy.*, **34**, 606-628.

Tunaboyu, O. and Avşar, Ö. (2017), "Seismic repair of captive-column damage with CFRPs in substandard RC frames", *Struct. Eng. Mech.*, **61**(1), 1-13.

Turkish Earthquake Code (2007), *Specification for Buildings to be Built in Seismic Zones*, Ministry of Public Works and Settlement Government of Republic of Turkey, Ankara, Turkey.

Wang, L., Xuan, W., Zhang, Y., Cong, S., Liu, F., Gao, Q. and Chen, H. (2016), "Experimental and numerical research on seismic performance of earthquake-damaged RC frame strengthened with CFRP sheets", *Adv. Mater. Sci. Eng.*

Yang, Y., Sneed, L.H., Saiidi, M.S., Belarbi, A., Ehsani, M. and He, R. (2015), "Emergency repair of an earthquake-damaged RC bridge column with fractured bars using externally bonded prefabricated laminates-an experimental study", *Compos. Struct.*, **133**, 727-738.

Yılmaz, N. and Avsar, Ö. (2013), "Structural damages of the May 19, 2011 Kütahya-Simav earthquake in Turkey", *Nat. Haz.*, **69**(1), 981-1001.

CC